

Generating Novel, Designable, and Diverse Protein Structures by Equivariantly Diffusing Oriented Residue Clouds

Yeqing Lin^{1,2} Mohammed AlQuraishi^{1,2}

Abstract

Proteins power a vast array of functional processes in living cells. The capability to create new proteins with designed structures and functions would thus enable the engineering of cellular behavior and development of protein-based therapeutics and materials. Structure-based protein design aims to find structures that are designable (can be realized by a protein sequence), novel (have dissimilar geometry from natural proteins), and diverse (span a wide range of geometries). While advances in protein structure prediction have made it possible to predict structures of novel protein sequences, the combinatorially large space of sequences and structures limits the practicality of search-based methods. Generative models provide a compelling alternative, by implicitly learning the low-dimensional structure of complex data distributions. Here, we leverage recent advances in denoising diffusion probabilistic models and equivariant neural networks to develop Genie, a generative model of protein structures that performs discrete-time diffusion using a cloud of oriented reference frames in 3D space. Through *in silico* evaluations, we demonstrate that Genie generates protein backbones that are more designable, novel, and diverse than existing models. This indicates that Genie is capturing key aspects of the distribution of protein structure space and facilitates protein design with high success rates.

taking diversity of protein structures and accordant functions. Yet, relative to the full potential size of foldable protein space, evolution has only explored a small subregion (Huang et al., 2016). This leaves open the possibility of designing new proteins unlike any seen in nature, if suitable algorithms can be developed that correctly model uncharted parts of fold space.

Protein design efforts historically focused on optimizing functional properties of naturally occurring proteins through directed evolution (Dougherty & Arnold, 2009) or through rational design of novel protein sequences that hew closely to known structural motifs (Kuhlman et al., 2003). This limited exploration of fold space to regions adjacent to naturally occurring proteins. With recent advances in protein structure prediction methods, new approaches have been proposed that leverage representations learned by these methods to more broadly explore structure space. For example, Anishchenko et al. (2021) performed Monte Carlo sampling in sequence space using trRosetta (Yang et al., 2020) as a guide and were able to discover novel structures. One disadvantage of this approach however is the reliance on sampling, which can be computationally expensive and difficult to steer toward desirable design goals.

The development of generative models capable of capturing complex data distributions has provided a new direction for *de novo* protein design. Instead of sampling from protein sequence space, protein design could be achieved by implicitly learning the underlying space of structures. Generative modeling offers a number of paradigms, most of which developed and refined for image generation. Which paradigm is best suited for proteins, and how it should be adapted to their 3D world, are key outstanding questions.

1. Introduction

Proteins play an essential role in all cellular processes, ranging from chemical catalysis to molecular transport. Over the course of evolution, nature has explored a breath-

Generative modeling trilemma Generative models generally contend with a trilemma in optimizing between generation quality (in the protein context, physicality and designability), mode coverage (novelty and diversity of generated structures) and sampling time (Xiao et al., 2022). Multiple modeling paradigms exist, each making a different trade-off. Generative Adversarial Networks (GANs) (Goodfellow et al., 2014) pit two neural networks in competition with one another—a generator network that creates

¹Department of Computer Science, Columbia University, New York, NY, USA ²Department of Systems Biology, Columbia University, New York, NY, USA. Correspondence to: Mohammed AlQuraishi <m.alquraishi@columbia.edu>.

new data instances and a discriminator network that distinguishes between real and generated instances. Through this process, GANs learn to map a simple latent space defined by *e.g.*, a multivariate Gaussian distribution to the complex space that implicitly captures, in part, the underlying data distribution. GANs are capable of rapid generation of high quality samples but suffer from unstable training and mode collapse in which parts of the data distribution are left uncaptured (Brock et al., 2019; Karras et al., 2020; Zhao et al., 2021). Variational AutoEncoders (VAEs) (Kingma & Welling, 2013) are likelihood-based generative models that learn a low-dimensional latent space through reconstruction. More specifically, they consist of two separate networks, an encoder that maps data instances into a low-dimensional latent space and a decoder that reconstructs data instances from their corresponding latent representations. By minimizing a variational lower bound, VAEs aim to maximize the probability of observed data. In practice, VAEs achieve good mode coverage but produce lower quality samples (van den Oord et al., 2017; Razavi et al., 2019).

More recently, denoising diffusion probabilistic models (DDPMs) (Ho et al., 2020; Nichol & Dhariwal, 2021) have shown considerable promise in generating high quality 2D images, as exemplified by DALL-E 2 (Ramesh et al., 2022) and Stable Diffusion (Rombach et al., 2022). DDPMs consist of a forward process that iteratively adds a small amount of Gaussian noise to a sample, and a reverse process that iteratively removes noise from a noisy sample. DDPMs optimize for sample quality and diversity, achieving state-of-the-art performance on both (Dhariwal & Nichol, 2021). However, they suffer from a slow sampling process, as generation proceeds through a denoising process that repeatedly executes computationally-intensive inference. Nonetheless, because of the notably higher quality and diversity of generated samples, DDPMs have become the generative paradigm of choice for images.

Application to protein design Multiple prior efforts have applied generative modeling to structure-based protein design. The first generation of methods parameterized protein geometry using inter-residue distances, leveraging the pre-existing machinery for 2D image generation. For instance, Anand and Huang (2018) used GANs to generate pairwise distance matrices of C_α atoms in proteins, followed by convex optimization to reconstruct the corresponding 3D coordinates. Anand et al. (2019) later introduced an additional refinement network to improve coordinate reconstruction. One limitation of this approach is the lack of a guarantee that generated pairwise distances are embeddable in 3D space, leading to potential inconsistencies between raw samples (in distance matrix space) and generated coordinates. Errors in distance matrices often lead to significant deterioration in structural quality (Eguchi et al., 2022), and prevent the model from being

optimized in an end-to-end fashion for final 3D geometry.

An alternate parameterization for protein structure can be formulated using internal coordinates, where torsion angles between adjacent residues are used to encode 3D geometry. This approach sidesteps the embeddability problem of distance-based representations, but may be overly reliant on reasoning over local protein geometry (AlQuraishi, 2019). One example is FoldingDiff (Wu et al., 2022a), which performs diffusion in the space of internal coordinates using a bidirectional transformer with relative positional embeddings to iteratively denoise a sequence of torsion angles. FoldingDiff yields protein-like backbones, but the majority of generated structures are predicted to not be designable when assessed using *in silico* sequence-structure self-consistency metrics (described later). One possible reason for this is that errors in predicted internal coordinates can accumulate and propagate along the protein chain during the coordinate reconstruction process.

A third approach parameterizes proteins using atomic coordinates in Cartesian space. Unlike distance-based and internal coordinate parameterizations, this approach is not inherently invariant to rotations and translations (SE(3)-invariance). As proteins do not have preferred orientations or locations, capturing these invariances would improve the data efficiency of the generative model (Anand & Achim, 2022). Recent developments in geometric neural networks, including EGNN (Satorras et al., 2021) and GVP (Jing et al., 2021), provide powerful tools for geometric reasoning in an SE(3)-equivariant manner. Employing EGNNs for this purpose, Trippe et al. (2022) developed ProtDiff, a DDPM that directly generates the C_α coordinates of protein structures. Although a promising approach, ProtDiff struggles to produce geometries with realizable protein sequences. One potential reason for this is the reflection-invariant property of EGNNs, which is non-physical and frequently yields left-handed alpha helices, an exceedingly rare structural element in real proteins.

In protein structure prediction, AlphaFold2 (Jumper et al., 2021) achieved great success by combining implicit reasoning in a latent space (evoformer module) with geometric reasoning in Cartesian space (structure module). A key feature of the latter is Invariant Point Attention (IPA), a mechanism for computationally-efficient, SE(3)-equivariant reasoning that is sensitive to reflections. IPA parameterizes proteins using rigid body frames anchored at residues, which can be defined in a consistent manner irrespective of global position or orientation by taking advantage of the polymeric nature of protein backbones. Using a cloud of reference frames, instead of a point cloud, retains angular information between residues and thus accounts for chemical chirality.

Here, we combine aspects of the SE(3)-equivariant rea-

soning machinery of IPA with DDPMs to create a diffusion process over protein backbone geometry in Cartesian space. Key to our approach is a geometric asymmetry in how protein residues are represented—as point clouds in the standard forward process of DDPMs (the noising procedure) and as a cloud of reference frames in the reverse process (sample generation procedure). This enables us to use a simple and cheap process for noising structures while retaining the full expressivity of IPA during generation. The resulting model, Genie, is capable of generating diverse structures that are simultaneously designable and novel. Through *in silico* comparisons with leading methods, we show that Genie achieves state-of-the-art performance on key design metrics. Contemporaneous with this work, two other methods reported highly performant DDPMs for protein design inspired by similar ideas (Ingraham et al., 2022; Watson et al., 2022), although their architectural details and training procedures are distinct from Genie.

2. Methods

Genie is a DDPM that generates protein backbones as a sequence of C_α atomic coordinates. It performs diffusion directly in Cartesian space and uses an SE(3)-equivariant denoiser that reasons over a cloud of reference frames to predict noise displacements at each diffusion step. In Section 2.1, we describe our tailored implementation of DDPMs for protein backbone generation. In Section 2.2, we provide details on the SE(3)-equivariant denoiser. In Sections 2.3 and 2.4, we describe how we train and sample from the model, respectively.

2.1. Denoising Diffusion Probabilistic Model

Let $\mathbf{x} = [\mathbf{x}^1, \mathbf{x}^2, \dots, \mathbf{x}^N]$ denote a sequence of C_α coordinates of length N , corresponding to a protein with N residues. Given a sample \mathbf{x}_0 from the unknown data distribution over protein structures, the forward process iteratively adds isotropic Gaussian noise to the sample following a cosine variance schedule $\beta = [\beta_1, \beta_2, \dots, \beta_T]$:

$$q(\mathbf{x}_t | \mathbf{x}_{t-1}) = \mathcal{N}(\mathbf{x}_t | \sqrt{1 - \beta_t} \mathbf{x}_{t-1}, \beta_t \mathbf{I}) \quad (1)$$

By reparameterization, we have

$$q(\mathbf{x}_t | \mathbf{x}_0) = \mathcal{N}(\mathbf{x}_t | \sqrt{\bar{\alpha}_t} \mathbf{x}_0, (1 - \bar{\alpha}_t) \mathbf{I}) \quad (2)$$

where

$$\bar{\alpha}_t = \prod_{s=1}^t \alpha_s \quad \text{and} \quad \alpha_t = 1 - \beta_t$$

Since the isotropic Gaussian noise added at each diffusion step is small, the reverse process can be modeled as a Gaussian process:

$$p(\mathbf{x}_{t-1} | \mathbf{x}_t) = \mathcal{N}(\mathbf{x}_{t-1} | \boldsymbol{\mu}_\theta(\mathbf{x}_t, t), \boldsymbol{\Sigma}_\theta(\mathbf{x}_t, t) \mathbf{I}) \quad (3)$$

where

$$\begin{aligned} \boldsymbol{\mu}_\theta(\mathbf{x}_t, t) &= \frac{1}{\sqrt{\alpha_t}} \left(\mathbf{x}_t - \frac{\beta_t}{\sqrt{1 - \bar{\alpha}_t}} \boldsymbol{\epsilon}_\theta(\mathbf{x}_t, t) \right) \\ \boldsymbol{\Sigma}_\theta(\mathbf{x}_t, t) &= \beta_t \end{aligned}$$

By starting the reverse process from pure white noise and then iteratively removing noise, Genie generates protein backbones *de novo*. Figure 1 illustrates diffusion of a protein backbone. Running the reverse process requires evaluating $\boldsymbol{\epsilon}_\theta(\mathbf{x}_t, t)$, which predicts the noise added at time step t . We model this using a novel geometric noise predictor that forms the core of our model.

2.2. Noise Prediction

In Genie, the noise predictor first takes the C_α coordinates at diffusion step t , denoted by \mathbf{x}_t , and computes discrete Frenet-Serret (FS) frames based on the backbone geometry encoded by \mathbf{x}_t . Each FS frame represents the position and orientation of a residue relative to the global reference frame. Once constructed, these FS frames enable downstream model components, including IPA, to reason about the relative orientations of protein residues and parts. FS frames are passed together with a sinusoidal encoding of diffusion step t to an SE(3)-invariant encoder and an SE(3)-equivariant decoder to compute a new set of FS frames, from which updated coordinates are extracted (see Appendix A.1 for more details). Noise is then computed as a set of displacement vectors between the original and updated coordinates, which is the final prediction of $\boldsymbol{\epsilon}_\theta(\mathbf{x}_t, t)$. Figure 2 summarizes Genie’s architecture.

FS frame construction Following Hu et al. (2011) and Chowdhury et al. (2022), we construct discrete FS frames \mathbf{F} as

$$\begin{aligned} \mathbf{t}^i &= \frac{\mathbf{x}^{i+1} - \mathbf{x}^i}{\|\mathbf{x}^{i+1} - \mathbf{x}^i\|} \\ \mathbf{b}^i &= \frac{\mathbf{t}^{i-1} \times \mathbf{t}^i}{\|\mathbf{t}^{i-1} \times \mathbf{t}^i\|} \\ \mathbf{n}^i &= \mathbf{b}^i \times \mathbf{t}^i \\ \mathbf{R}^i &= [\mathbf{t}^i, \mathbf{b}^i, \mathbf{n}^i] \\ \mathbf{F}^i &= (\mathbf{R}^i, \mathbf{x}^i) \end{aligned}$$

where the first element of \mathbf{F}^i is the rotation matrix and the second element is the translation vector. To handle the edge cases corresponding to the N- and C-termini of proteins, we assign the frames of the second and second-to-last residues to the first and last residues, respectively.

SE(3)-invariant encoder Given frames \mathbf{F}_t and the sinusoidal encoding of the corresponding diffusion step t , the encoder generates and refines single residue and paired residue-residue representations, which are used later by the

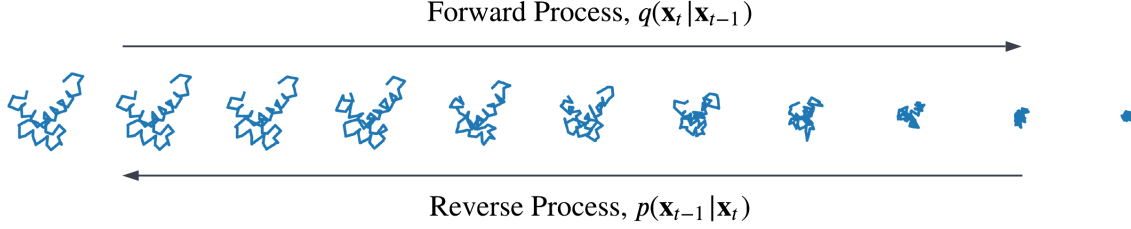


Figure 1. Diffusion of protein backbone in Cartesian space. The forward process iteratively adds isotropic Gaussian noise to C_α coordinates, while the reverse process iteratively denoises noisy coordinates through an SE(3)-equivariant model.

decoder to update the structure. As illustrated in Figure 2 (“Invariant Encoder”), the Single Feature Network first creates per residue representations (\mathbf{s}_t) from sinusoidal encodings of residue indices and the diffusion step. The Pair Feature Network then computes paired residue-residue representations (\mathbf{p}_t) from the outer sum of the (single) residue representations, relative positional encodings of residue pairs, and a pairwise distance matrix representation of the structure (based on C_α coordinates). These pair representations \mathbf{p}_t are iteratively refined in the Pair Transform Network using triangular multiplicative updates (Jumper et al., 2021). The encoder is SE(3)-invariant since both its single and pair representations are derived from SE(3)-invariant features. Appendix A.2 provides further details on the encoder.

SE(3)-equivariant decoder Given frames \mathbf{F}_t and the single (\mathbf{s}_t) and pair representations (\mathbf{p}_t) from the encoder, the decoder iteratively refines the structure by operating over \mathbf{F}_t in an SE(3)-equivariant manner. As illustrated in Figure 2 (“Equivariant Decoder”), the decoder first uses IPA to generate a new single representation \mathbf{s}'_t based on \mathbf{F}_t , \mathbf{s}_t , and \mathbf{p}_t . Here, frames are initialized using \mathbf{F}_t in lieu of the “black hole” initialization used by AlphaFold2. The Backbone Update Network then computes and applies frame updates based on the updated single representation \mathbf{s}'_t , resulting in a new set of frames \mathbf{F}'_t . The decoder is SE(3)-equivariant since frame updates are computed based on the SE(3)-invariant \mathbf{s}'_t . Thus, any global transformation of the input frames is also applied to the final output frames.

Noise prediction Given the input coordinates \mathbf{x}_t and the updated frames \mathbf{F}'_t , we extract the updated coordinates \mathbf{x}'_t from the translation component of \mathbf{F}'_t and compute the predicted noise $\epsilon_\theta(\mathbf{x}_t, t)$ as $\mathbf{x}_t - \mathbf{x}'_t$.

2.3. Training

Since the forward diffusion process is predefined with a fixed variance schedule, training Genie essentially reduces to training the noise prediction model. By minimizing the error in noise prediction for each diffusion step, Genie learns to iteratively reverse the diffusion process and gener-

ate novel protein backbones. For this work, we consider a maximum sequence length of 128. Appendix A.3 provides more details on the training process.

Loss Following Ho et al. (2020), which found that diffusion models achieve better performance when using noise ϵ_t as the prediction target instead of the mean in the reverse probability distribution $p(\mathbf{x}_{t-1}|\mathbf{x}_t)$, we define our loss as:

$$\begin{aligned} L &= \mathbb{E}_{t, \mathbf{x}_0, \epsilon} \left[\sum_{i=1}^N \|\epsilon_t - \epsilon_\theta(\mathbf{x}_t, t)\|^2 \right] \\ &= \mathbb{E}_{t, \mathbf{x}_0, \epsilon} \left[\sum_{i=1}^N \|\epsilon_t - \epsilon_\theta(\sqrt{\alpha_t} \mathbf{x}_0 + \sqrt{1 - \alpha_t} \epsilon_t, t)\|^2 \right] \end{aligned}$$

At each training step, we sample a protein domain x_0 from the training dataset, a diffusion step t from a uniform distribution of integers between 1 and T , and noise vectors ϵ_t from a unit Gaussian, and update model weights in the direction of minimizing the sum of per residue L_2 distances between true and predicted noise vectors.

Dataset For training data we use structures of protein domains from the Structural Classification of Proteins — extended (SCOPe) dataset. Protein domains are filtered so that no two domains share more than 40% sequence identity, to ensure that the data is non-redundant and diverse. We also use the structural hierarchy defined by SCOPe to delineate protein domains along four major classes: all alpha proteins, all beta proteins, alpha and beta proteins (α/β), and alpha and beta proteins ($\alpha + \beta$). We remove domains with multiple chains and missing backbone atoms. Our resulting training set comprises 8,766 domains, with 3,942 domains having at most 128 residues.

2.4. Sampling

To generate a new protein backbone of length N , we first sample a random sequence $\mathbf{x}_T = [\mathbf{x}_T^1, \mathbf{x}_T^2, \dots, \mathbf{x}_T^N]$ of C_α coordinates drawn from $\mathbf{x}_T^i \sim \mathcal{N}(\mathbf{0}, \mathbf{I})$ for all $i \in [1, N]$. This sequence of coordinates \mathbf{x}_T is then recursively fed through the reverse diffusion process until diffusion step

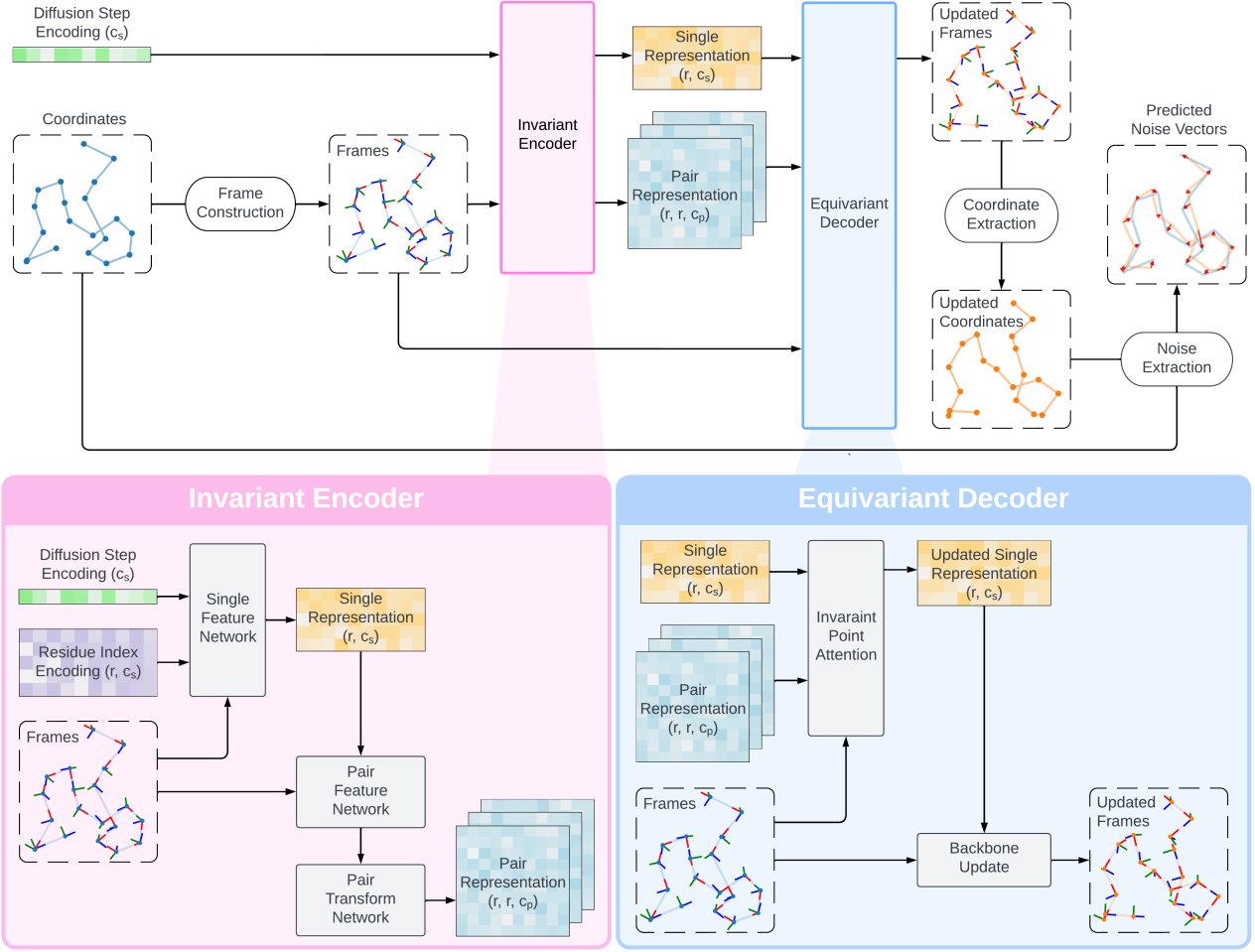


Figure 2. Architecture of SE(3)-equivariant denoiser, including SE(3)-invariant encoder (bottom left) and SE(3)-equivariant decoder (bottom right). Notation: r : number of residues, c_s : dimensionality of single representation, c_p : dimensionality of pair representation.

0 is reached. Using Equation 3, the update rule is:

$$\mathbf{x}_{t-1} = \begin{cases} \boldsymbol{\mu}_\theta(\mathbf{x}_t, t) + \sqrt{\boldsymbol{\Sigma}_\theta(\mathbf{x}_t, t)} \cdot \boldsymbol{\epsilon}, & \text{if } t > 1 \\ \boldsymbol{\mu}_\theta(\mathbf{x}_t, t), & \text{otherwise} \end{cases}$$

where $\boldsymbol{\epsilon} = [\epsilon^1, \epsilon^2, \dots, \epsilon^N]$ and each ϵ^i is drawn from a unit Gaussian distribution.

3. Results

To evaluate Genie, we generate 10 proteins for each sequence length between 50 and 128 residues and assess the resulting structures on designability, diversity, and novelty. We compare the performance of Genie on these criteria with ProtDiff and FoldingDiff, two recent diffusion models described earlier, and find that it outperforms both on all three criteria (see Appendix A.4 for more details).

3.1. Designability

The first assessment criterion we consider is designability, *i.e.*, the realizability of a generated backbone structure by a designed protein sequence. We follow the self-consistency Template Modeling (scTM) approach proposed by Trippe et al. (2022). Although purely an *in silico* method, it has shown promise in correctly identifying designable structures (Dauparas et al., 2022). Briefly, scTM takes a generated backbone structure and feeds it into ProteinMPNN, a state-of-the-art structure-conditioned sequence generation method. Using ProteinMPNN set at a sampling temperature of 0.1, we generate eight sequences per input structure and then use OmegaFold (Wu et al., 2022b) to predict the structure of each putative sequence. The original scTM approach used AlphaFold2 but we substitute OmegaFold for AlphaFold2 as it outperforms the latter on single-sequence structure prediction (we also employ ESMFold (Lin et al.,

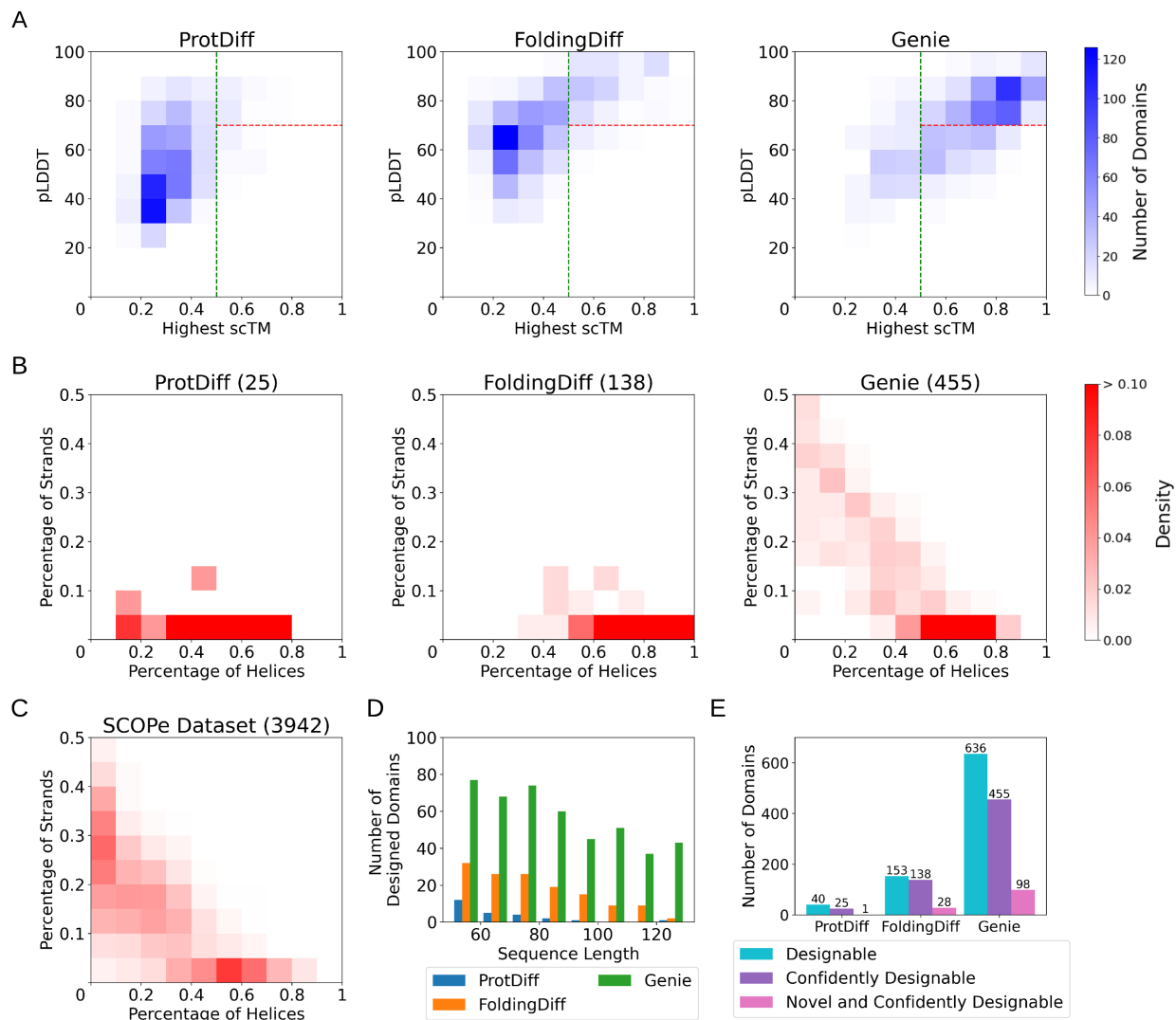


Figure 3. Evaluation results. (A) Heatmap of the relative frequencies of generated domains with specific combinations of highest scTM and pLDDT values achieved by ProtDiff, FoldingDiff, and Genie. (B) Heatmap of relative frequencies of confidently designable domains with specific combinations of fractional SSE content. The number of designed domains for each model is shown in parentheses. (C) Heatmap of relative frequencies of our SCOPe dataset. This diagram uses the same color scheme as (B) and is provided for reference. (D) Histogram of confidently designable domains as a function of sequence length. (E) Bar chart of number of designable domains generated by different methods out of a fixed budget of 780 attempted designs per method.

2022) for the same purpose and observe similar trends — see Appendix C). Finally, we compute scTM by measuring the TM-score (Zhang & Skolnick, 2004) — a metric of structural congruence — of the OmegaFold-predicted structure with respect to the original generated structure. scTM scores range from 0 to 1 with higher numbers corresponding to increased likelihoods that an input structure is designable. Appendix B provides an illustration of the scTM pipeline.

For each protein structure generated by each method, we compute the highest scTM score achieved across the eight

putative sequences and the predicted local distance difference test score averaged across all residues (pLDDT) for the designed structure with the highest scTM score. pLDDT is an OmegaFold-derived score (initially introduced by AlphaFold2) that summarizes OmegaFold’s own confidence in its predictions, ranging in value from 0 to 100 with $\text{pLDDT} > 70$ corresponding to confident predictions. Figure 3A shows the distribution of highest scTM scores versus pLDDTs for all three models. Similar to previous work (Trippe et al., 2022; Wu et al., 2022a), we first use $\text{scTM} > 0.5$ as a cutoff for designability since it sug-

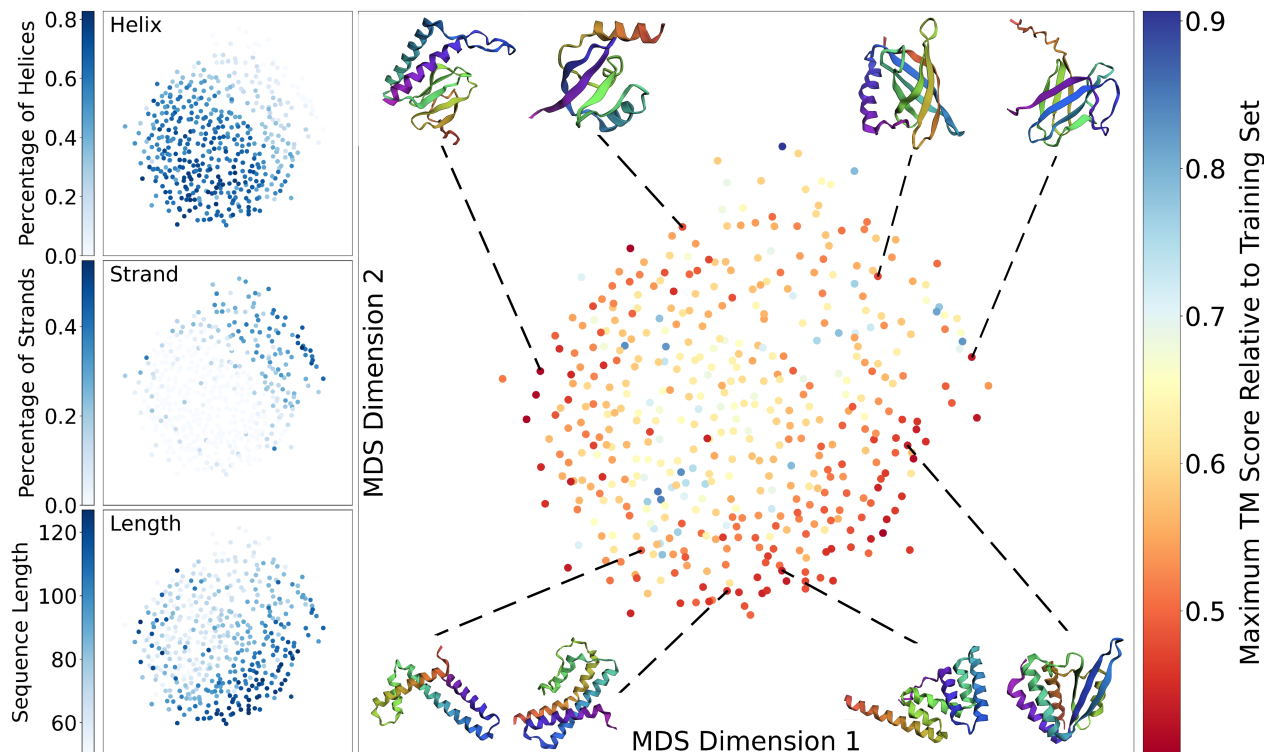


Figure 4. Design space of Genie. 455 Genie-generated structures that are confidently designable were embedded in 2D space using multidimensional scaling (MDS) with pairwise TM scores as the distance metric. Domains are colored by their maximum TM score to the training set (central panel), fraction of helical residues (top left panel), fraction of beta strand residues (middle left panel), and sequence length (bottom left panel). Eight novel designed domains are shown as representatives.

gests that the generated and designed structures are of the same general fold (Xu & Zhang, 2010). 81.5% of protein domains generated by Genie have $scTM > 0.5$, far exceeding the percentages for ProtDiff (5.1% and 11.8% for re-trained and reported models, respectively) and FoldingDiff (19.6% and 22.7% for resampled and reported results, respectively). This indicates that on average Genie generates more designable protein structures.

While $scTM$ reflects a model’s ability to find structures with designable sequences, it leaves open the possibility that OmegaFold-predicted structures are of insufficient quality to be used reliably in computing $scTM$ scores. We thus place an additional constraint that predicted structures achieve $pLDDT > 70$ to enrich for confidently-predicted structures. When considering both criteria, 58.3% of domains generated by Genie are designable with confidently-predicted structures (henceforth, “confidently designable”), while only 3.2% and 17.7% of ProtDiff- and FoldingDiff-generated domains are, respectively. Figure 3D shows the distribution of confidently designed structures binned by sequence length. We observe that Genie outperforms ProtDiff and FoldingDiff across short and long proteins. Furthermore, Genie-generated structures universally satisfy physical chirality constraints while those gen-

erated by ProtDiff often contain left-handed helices.

3.2. Diversity

The second assessment criterion we consider is the diversity of generated structures. We first evaluate diversity by considering the relative proportion of secondary structure elements (SSEs) in generated domains. SSEs are local patterns of structure within proteins that are characterized by specific types of hydrogen bonding networks. The most common types of SSEs are α -helices and β -strands, and we focus on these in our assessments.

To identify SSEs in generated structures, we use the Protein Secondary Element Assignment (P-SEA) algorithm (Labesse et al., 1997). P-SEA detects SSEs using a set of hand-crafted rules based on distances and angles between consecutive C_α atoms in protein backbones. We applied P-SEA to all confidently designable structures ($scTM > 0.5$; $pLDDT > 70$). Figure 3B shows the relative frequencies of designed domains with different fractions of SSEs and Figure 3C provides the baseline frequencies of our SCOPe dataset for reference. Domains generated by FoldingDiff and ProtDiff are dominated by mainly α -helical domains, with only 2 (out of 25, 8%) and 10 (out of 138, 7.25%)

of their designs containing β -strands, respectively. In contrast, Genie designs are more diverse, with 254 mainly α -helical, 25 mainly β -strand, and 176 α, β -mixed domains.

In addition to SSE content, we assess the diversity of tertiary structures in confidently designed domains. For each domain, we compute its maximum TM score to all other confidently designed domains, which quantifies its similarity to the most structurally similar domain in the designed set. For a diverse set of domains, most domains should have small maximum TM scores to all other domains. Genie achieves, on average, a maximum TM score of 0.561 ± 0.086 relative to the designed set, which is lower than both ProtDiff (0.583 ± 0.115) and FoldingDiff (0.668 ± 0.178). This suggests that Genie-designed domains are more diverse and better able to capture the fold distribution of protein structure space.

3.3. Novelty

The third assessment criterion we consider is the novelty of generated protein structures. As a major goal of protein design is the creation of new protein folds and geometries, novelty is a key feature of any structure-based protein design tool. To quantify the novelty of generated structures we compute their maximum TM scores with respect to all structures in the training set. We use the TM-Align software package for this purpose (Zhang & Skolnick, 2004). To classify a confidently designable domain as novel, we require that its maximum TM score to the training set is less than 0.5 — a widely used heuristic for determining when two protein domains are of dissimilar folds. Using this criterion, we find that 98 out of 455 (21.5%) confidently designable structures generated by Genie are novel, relative to 4% (1 out of 25) and 20.3% (28 out of 138) for ProtDiff and FoldingDiff, respectively. Figure 3E summarizes the statistics on generated domains for all three models.

To visualize the design space of Genie, we apply multi-dimensional scaling (MDS) to the pairwise TM scores of all 455 confidently designable domains and show the resulting 2D space in Figure 4. By overlaying maximum TM scores (relative to the training set) and SSE content on the MDS embedding, we confirm that Genie can generate diverse protein domains. We further observe that this diversity is evenly distributed throughout the embedding, with some localization of beta-dominated domains. We illustrate the quality and diversity of generated domains by showing eight novel designs chosen from diverse embedding locations. Appendix D provides additional visualizations of novel domains.

4. Conclusion

In this work, we present Genie, a novel DDPM for *de novo* protein design that substantially outperforms previous structure-based methods. One important contributing factor to Genie’s success is the use of dual representations for protein residues. By representing a protein as a sequence of C_α coordinates in Cartesian space instead of FS frames, we can perform diffusion by injecting isotropic Gaussian noise into C_α coordinates, bypassing the need to noise rotation matrices, a more delicate task. On the other hand, during noise prediction, proteins are represented as sequences of FS frames, allowing Genie to reason about inter-residue orientations and achieve better structural quality. Thus we simultaneously achieve simplicity of design and geometric expressiveness. Practically, noise prediction is accomplished by combining IPA with backbone updates, which provide a powerful way to reason spatially about protein structure, maintaining equivariance to both translations and rotations while being sensitive to reflections.

Future directions for this work center around two key areas. The first is to expand Genie to include a sequence generation module, allowing it to perform *de novo* sequence-structure design. By learning to generate sequence and structure concurrently, the model may better capture the space of foldable proteins and achieve greater success at designing novel proteins. Additional architectural improvements may also be necessary to enable efficient training of Genie and generation of larger proteins.

The second area is to facilitate application of Genie to biologically functional designs. Genie’s success in unconditional structure generation immediately indicates its potential for conditional generation based on structural or functional properties. Such conditional generation has been achieved by other methods, for example in producing protein structures that contain functional sites (Wang et al., 2022). The use of pretrained classifiers (*e.g.*, function classifiers) to guide the DDPM generation process towards novel proteins with desired properties is particularly promising, including in drug discovery. Contemporaneous methods (Ingraham et al., 2022; Watson et al., 2022) have shown promise in this direction and we hope that the innovations introduced by Genie will further drive progress.

References

- Ahdritz, G., Bouatta, N., Kadyan, S., Xia, Q., Gerecke, W., O’Donnell, T. J., Berenberg, D., Fisk, I., Zanichelli, N., Zhang, B., Nowaczynski, A., Wang, B., Stepniewska-Dziubinska, M. M., Zhang, S., Ojewole, A., Guney, M. E., Biderman, S., Watkins, A. M., Ra, S., Lorenzo, P. R., Nivon, L., Weitzner, B., Ban, Y.-E. A., Sorger, P. K., Mostaque, E., Zhang, Z., Bonneau, R., and

- AlQuraishi, M. Openfold: Retraining AlphaFold2 yields new insights into its learning mechanisms and capacity for generalization. *bioRxiv*, 2022. doi: 10.1101/2022.11.20.517210.
- AlQuraishi, M. End-to-end differentiable learning of protein structure. *Cell Systems*, 8(4):292–301, 2019.
- Anand, N. and Achim, T. Protein structure and sequence generation with equivariant denoising diffusion probabilistic models. *arXiv preprint arXiv:2205.15019*, 2022.
- Anand, N. and Huang, P.-S. Generative modeling for protein structures. *Advances in Neural Information Processing Systems*, 31, 2018.
- Anand, N., Eguchi, R. R., and Huang, P.-S. Fully differentiable full-atom protein backbone generation. In *DGS@ICLR*, 2019.
- Anishchenko, I., Pellock, S. J., Chidyausiku, T. M., Ramelot, T. A., Ovchinnikov, S., Hao, J., Bafna, K., Norn, C., Kang, A., Bera, A. K., DiMaio, F., Carter, L., Chow, C. M., Montelione, G. T., and Baker, D. De novo protein design by deep network hallucination. *Nature*, 600(7889):547–552, 2021.
- Brock, A., Donahue, J., and Simonyan, K. Large scale gan training for high fidelity natural image synthesis. In *International Conference on Learning Representations*, 2019.
- Chowdhury, R., Bouatta, N., Biswas, S., Floristean, C., Kharkar, A., Roy, K., Rochereau, C., Ahdritz, G., Zhang, J., Church, G. M., Sorger, P. K., and AlQuraishi, M. Single-sequence protein structure prediction using a language model and deep learning. *Nature Biotechnology*, pp. 1–7, 2022.
- Dauparas, J., Anishchenko, I., Bennett, N., Bai, H., Ragotte, R. J., Milles, L. F., Wicky, B. I. M., Courbet, A., de Haas, R. J., Bethel, N., Leung, P. J. Y., Huddy, T. F., Pellock, S., Tischer, D., Chan, F., Koepnick, B., Nguyen, H., Kang, A., Sankaran, B., Bera, A. K., King, N. P., and Baker, D. Robust deep learning-based protein sequence design using ProteinMPNN. *Science*, 378(6615):49–56, 2022.
- Dhariwal, P. and Nichol, A. Diffusion models beat GANs on image synthesis. *Advances in Neural Information Processing Systems*, 34:8780–8794, 2021.
- Dougherty, M. J. and Arnold, F. H. Directed evolution: new parts and optimized function. *Current Opinion in Biotechnology*, 20(4):486–491, 2009.
- Eguchi, R. R., Choe, C. A., and Huang, P.-S. Ig-VAE: Generative modeling of protein structure by direct 3D coordinate generation. *PLoS computational biology*, 18(6): e1010271, 2022.
- Goodfellow, I., Pouget-Abadie, J., Mirza, M., Xu, B., Warde-Farley, D., Ozair, S., Courville, A., and Bengio, Y. Generative adversarial nets. *Advances in Neural Information Processing Systems*, 27, 2014.
- Ho, J., Jain, A., and Abbeel, P. Denoising diffusion probabilistic models. *Advances in Neural Information Processing Systems*, 33:6840–6851, 2020.
- Hu, S., Lundgren, M., and Niemi, A. J. Discrete frenet frame, inflection point solitons, and curve visualization with applications to folded proteins. *Physical Review E*, 83(6):061908, 2011.
- Huang, P.-S., Boyken, S. E., and Baker, D. The coming of age of de novo protein design. *Nature*, 537(7620): 320–327, 2016.
- Ingraham, J., Baranov, M., Costello, Z., Frappier, V., Ismail, A., Tie, S., Wang, W., Xue, V., Obermeyer, F., Beam, A., and Grigoryan, G. Illuminating protein space with a programmable generative model. *bioRxiv*, 2022. doi: 10.1101/2022.12.01.518682.
- Jing, B., Eismann, S., Suriana, P., Townshend, R. J., and Dror, R. O. Learning from protein structure with geometric vector perceptrons. In *International Conference on Learning Representations*, 2021.
- Jumper, J., Evans, R., Pritzel, A., Green, T., Figurnov, M., Ronneberger, O., Tunyasuvunakool, K., Bates, R., Židek, A., Potapenko, A., Bridgland, A., Meyer, C., Kohl, S. A. A., Ballard, A. J., Cowie, A., Romera-Paredes, B., Nikolov, S., Jain, R., Adler, J., Back, T., Petersen, S., Reiman, D., Clancy, E., Zielinski, M., Steinegger, M., Pacholska, M., Berghammer, T., Bodenstein, S., Silver, D., Vinyals, O., Senior, A. W., Kavukcuoglu, K., Kohli, P., and Hassabis, D. Highly accurate protein structure prediction with AlphaFold. *Nature*, 596(7873):583–589, 2021.
- Karras, T., Laine, S., Aittala, M., Hellsten, J., Lehtinen, J., and Aila, T. Analyzing and improving the image quality of StyleGAN. In *Proceedings of the IEEE/CVF Conference on Computer Vision and Pattern Recognition*, pp. 8110–8119, 2020.
- Kingma, D. P. and Welling, M. Auto-encoding variational bayes. *arXiv preprint arXiv:1312.6114*, 2013.
- Kuhlman, B., Dantas, G., Ireton, G. C., Varani, G., Stoddard, B. L., and Baker, D. Design of a novel globular protein fold with atomic-level accuracy. *Science*, 302(5649):1364–1368, 2003.

- Labesse, G., Colloc'h, N., Pothier, J., and Mornon, J.-P. P-SEA: a new efficient assignment of secondary structure from C_α trace of proteins. *Bioinformatics*, 13(3):291–295, 1997.
- Lin, Z., Akin, H., Rao, R., Hie, B., Zhu, Z., Lu, W., Smetanin, N., dos Santos Costa, A., Fazel-Zarandi, M., Sercu, T., Candido, S., et al. Language models of protein sequences at the scale of evolution enable accurate structure prediction. *bioRxiv*, 2022.
- Nichol, A. and Dhariwal, P. Improved denoising diffusion probabilistic models. In *International Conference on Machine Learning*, pp. 8162–8171. PMLR, 2021.
- Ramesh, A., Dhariwal, P., Nichol, A., Chu, C., and Chen, M. Hierarchical text-conditional image generation with CLIP latents. *arXiv preprint arXiv:2204.06125*, 2022.
- Razavi, A., van den Oord, A., and Vinyals, O. Generating diverse high-fidelity images with VQ-VAE-2. *Advances in Neural Information Processing Systems*, 32, 2019.
- Rombach, R., Blattmann, A., Lorenz, D., Esser, P., and Ommer, B. High-resolution image synthesis with latent diffusion models. In *Proceedings of the IEEE/CVF Conference on Computer Vision and Pattern Recognition*, pp. 10684–10695, 2022.
- Satorras, V. G., Hoogeboom, E., and Welling, M. E(n) equivariant graph neural networks. In *International Conference on Machine Learning*, pp. 9323–9332. PMLR, 2021.
- Trippe, B. L., Yim, J., Tischer, D., Baker, D., Broderick, T., Barzilay, R., and Jaakkola, T. Diffusion probabilistic modeling of protein backbones in 3d for the motif-scaffolding problem. *arXiv preprint arXiv:2206.04119*, 2022.
- van den Oord, A., Vinyals, O., and Kavukcuoglu, K. Neural discrete representation learning. *Advances in Neural Information Processing Systems*, 30, 2017.
- Wang, J., Lisanza, S., Juergens, D., Tischer, D., Watson, J. L., Castro, K. M., Ragotte, R., Saragovi, A., Milles, L. F., Baek, M., Anishchenko, I., Yang, W., Hicks, D. R., Expòsit, M., Schlichthaerle, T., Chun, J.-H., Dauparas, J., Bennett, N., Wicky, B. I. M., Muenks, A., DiMaio, F., Correia, B., Ovchinnikov, S., and Baker, D. Scaffolding protein functional sites using deep learning. *Science*, 377(6604):387–394, 2022.
- Watson, J. L., Juergens, D., Bennett, N. R., Trippe, B. L., Yim, J., Eisenach, H. E., Ahern, W., Borst, A. J., Ragotte, R. J., Milles, L. F., Wicky, B. I. M., Hanikel, N., Pellock, S. J., Courbet, A., Sheffler, W., Wang, J., Venkatesh, P., Sappington, I., Torres, S. V., Lauko, A., De Bortoli, V., Mathieu, E., Barzilay, R., Jaakkola, T. S., DiMaio, F., Baek, M., and Baker, D. Broadly applicable and accurate protein design by integrating structure prediction networks and diffusion generative models. *bioRxiv*, 2022. doi: 10.1101/2022.12.09.519842.
- Wu, K. E., Yang, K. K., Berg, R. v. d., Zou, J. Y., Lu, A. X., and Amini, A. P. Protein structure generation via folding diffusion. *arXiv preprint arXiv:2209.15611*, 2022a.
- Wu, R., Ding, F., Wang, R., Shen, R., Zhang, X., Luo, S., Su, C., Wu, Z., Xie, Q., Berger, B., Ma, J., and Peng, J. High-resolution de novo structure prediction from primary sequence. *bioRxiv*, 2022b.
- Xiao, Z., Kreis, K., and Vahdat, A. Tackling the generative learning trilemma with denoising diffusion GANs. In *International Conference on Learning Representations*, 2022.
- Xu, J. and Zhang, Y. How significant is a protein structure similarity with TM-score= 0.5? *Bioinformatics*, 26(7): 889–895, 2010.
- Yang, J., Anishchenko, I., Park, H., Peng, Z., Ovchinnikov, S., and Baker, D. Improved protein structure prediction using predicted interresidue orientations. *Proceedings of the National Academy of Sciences*, 117(3):1496–1503, 2020.
- Zhang, Y. and Skolnick, J. Scoring function for automated assessment of protein structure template quality. *Proteins: Structure, Function, and Bioinformatics*, 57(4): 702–710, 2004.
- Zhao, Z., Singh, S., Lee, H., Zhang, Z., Odena, A., and Zhang, H. Improved consistency regularization for GANs. In *Proceedings of the AAAI Conference on Artificial Intelligence*, volume 35, pp. 11033–11041, 2021.

A. Genie Architectural Details

A.1. Encodings

Sinusoidal encoding of diffusion step Let T denote the total number of diffusion steps and D denote the encoding dimension. We define the sinusoidal encoding of diffusion step t as

$$\phi(t) = \begin{bmatrix} f(t, 1) \\ f(t, 2) \\ \vdots \\ f(t, D) \end{bmatrix}$$

where

$$f(t, d) = \begin{cases} \sin\left(t \cdot \pi / T^{\frac{2 \cdot d}{D}}\right), & \text{if } d \bmod 2 = 0 \\ \cos\left(t \cdot \pi / T^{\frac{2 \cdot (d-1)}{D}}\right), & \text{otherwise} \end{cases}$$

Sinusoidal encoding of residue index Let N denote the maximum sequence length. We define the sinusoidal encoding of residue index n as

$$\phi(n) = \begin{bmatrix} f(n, 1) \\ f(n, 2) \\ \vdots \\ f(n, D) \end{bmatrix}$$

where

$$f(n, d) = \begin{cases} \sin\left(n \cdot \pi / N^{\frac{2 \cdot d}{D}}\right), & \text{if } d \bmod 2 = 0 \\ \cos\left(n \cdot \pi / N^{\frac{2 \cdot (d-1)}{D}}\right), & \text{otherwise} \end{cases}$$

Relative positional encoding We use a linear function to encode the k -clipped relative position between residue pairs. Given residue i and residue j , we first compute the clipped distance between residues in the amino acid sequence using

$$d(i, j) = \min(\max(i - j, -k), k)$$

We then compute a one-hot encoding of this clipped distance and use a linear function to project it to the same dimensionality as the pair representation. Residue pairs more than k residues apart are all assigned the same learned encoding.

A.2. SE(3)-Invariant Encoder

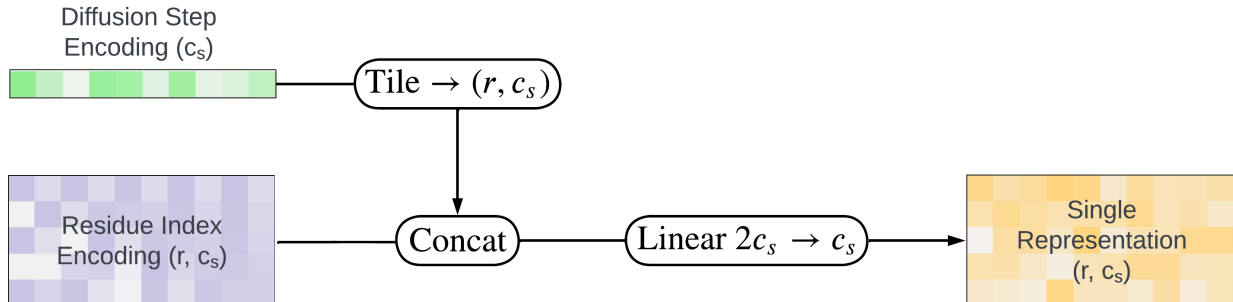


Figure 5. Architecture of the Single Feature Network, which generates single representations from sinusoidal encodings of the diffusion step and residue index. Notation: r : number of residues, c_s : dimension of single representation.

The SE(3)-invariant encoder constructs and refines single and pair representations based on input FS frames and a sinusoidal encoding of the diffusion step. We set the dimensionality of the single and pair representations to 128.

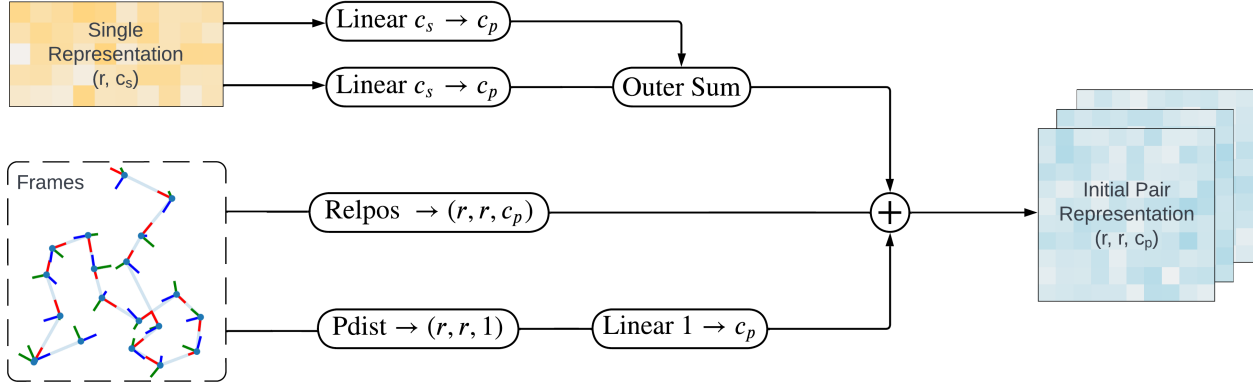


Figure 6. Architecture of the Pair Feature Network, which generates pair representations from the single representation and Frenet-Serret frames. Notation: r : number of residues, c_s : dimensionality of single representation, c_p : dimensionality of pair representation, $relpos$: relative positional encoding function, $pdist$: pairwise distance function.

Single Feature Network The Single Feature Network constructs the (single) residue representation s_i by concatenating the sinusoidal encoding of diffusion step t and the sinusoidal encoding of residue index i , followed by a linear projection to s_i (Figure 5).

Pair Feature Network The Pair Feature Network computes the pair representation p_{ij} by summing three latent pair representations – the relative positional encoding between residue i and j (Appendix A.1), the outer summation of the projections of single representations s_i and s_j , and the projection of the pairwise distance between residues i and j (Figure 6). The clipping length k for computing relative positional encodings is set to 32.

Pair Transform Network The Pair Transform Network uses 5 layers of triangular multiplicative updates (introduced in the evoformer module of AlphaFold2) to refine the pair representations, which are later used by the SE(3)-equivariant decoder to update the single representations and FS frames. We consider a graph over amino acid residues. For each triplet of nodes ijk in the graph, where i, j and k are residue indices, edge ij is updated by integrating information from its two adjacent edges ik and jk . Since each edge is directed, there are two symmetric updates: the “incoming” edge version which updates edge ij based on the representations of incoming edges ki and kj , and the “outgoing” edge version which updates edge ij based on the representations of outgoing edges ik and jk . We perform triangular multiplicative updates using both versions.

A.3. Training

Genie is implemented in PyTorch. For AlphaFold2-inspired components, such as triangular multiplicative updates and Invariant Point Attention, we adapted implementations from OpenFold (Ahdritz et al., 2022). To train Genie, we use an Adam optimizer with a learning rate of 10^{-4} . The model is trained using data parallelism on 12 A100 Nvidia GPUs with an effective batch size of 48. We train Genie for 50000 epochs (~ 9 days).

A.4. Evaluation

For evaluating ProtDiff we retrained the model on our filtered SCOPe dataset (described in 2.3) since the original training dataset and pretrained model weights are not publicly available. The retrained model achieves slightly worse results than the reported model, possibly due to differences in training and dataset size. For FoldingDiff, we use the original pretrained model to generate samples for evaluation.

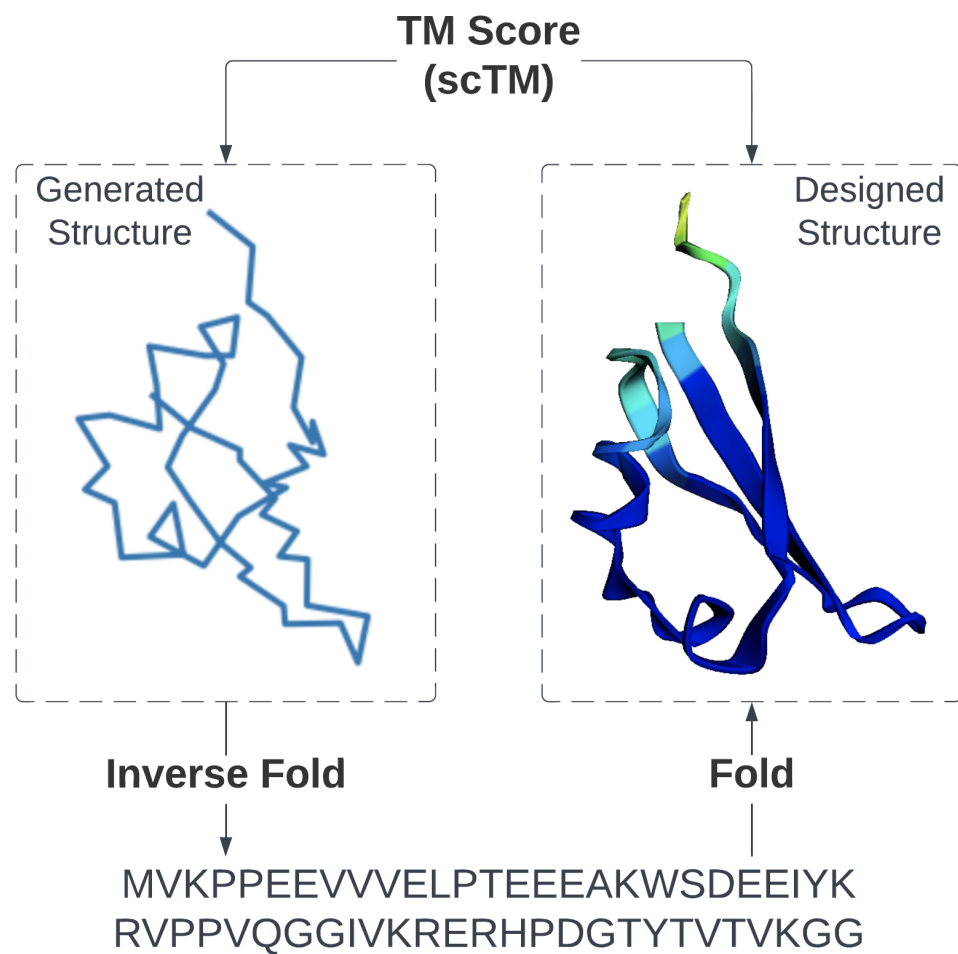
B. Illustration of scTM Pipeline

Figure 7. Self-consistency Template Modeling (scTM) pipeline. A generated structure is passed through an inverse folding model (*e.g.*, ProteinMPNN) to generate a sequence that is then passed to a protein structure prediction model (*e.g.*, AlphaFold2) to obtain the final designed structure. The scTM score is defined as the TM score between the generated and designed structures.

C. Extra Evaluations using ProteinMPNN-ESMFold scTM Pipeline

In Figure 8 we provide additional evaluations of Genie and other methods by replacing OmegaFold with ESMFold for protein structure prediction in scTM calculations. Overall trends remain unchanged from OmegaFold, except for an overall decrease in the number of confidently designable domains containing β -strands.

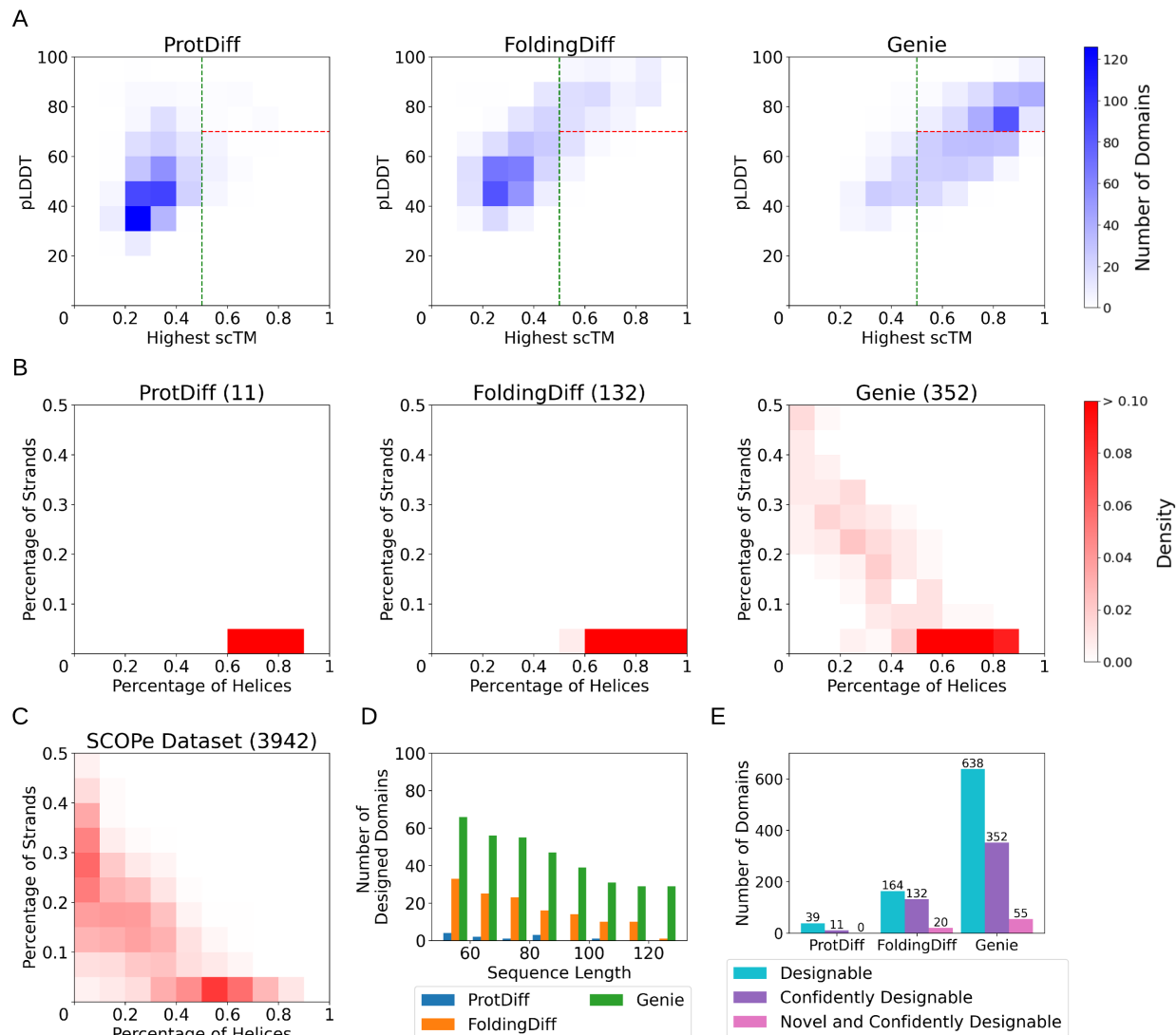


Figure 8. Evaluation results using ESMFold. (A) Heatmap of the relative frequencies of generated domains with specific combinations of highest scTM and pLDDT values achieved by ProtDiff, FoldingDiff, and Genie. (B) Heatmap of relative frequencies of confidently designable domains with specific combinations of fractional SSE content. The number of designed domains for each model is shown in parentheses. (C) Heatmap of relative frequencies of our SCOPe dataset. This diagram uses the same color scheme as (B) and is provided for reference. (D) Histogram of confidently designable domains as a function of sequence length. (E) Bar chart of number of designable domains generated by different methods out of a fixed budget of 780 attempted designs per method.

D. Visualizations of Genie-Generated Protein Backbones

We provide additional visualizations of Genie-generated domains that are confidently designable in Figure 9.

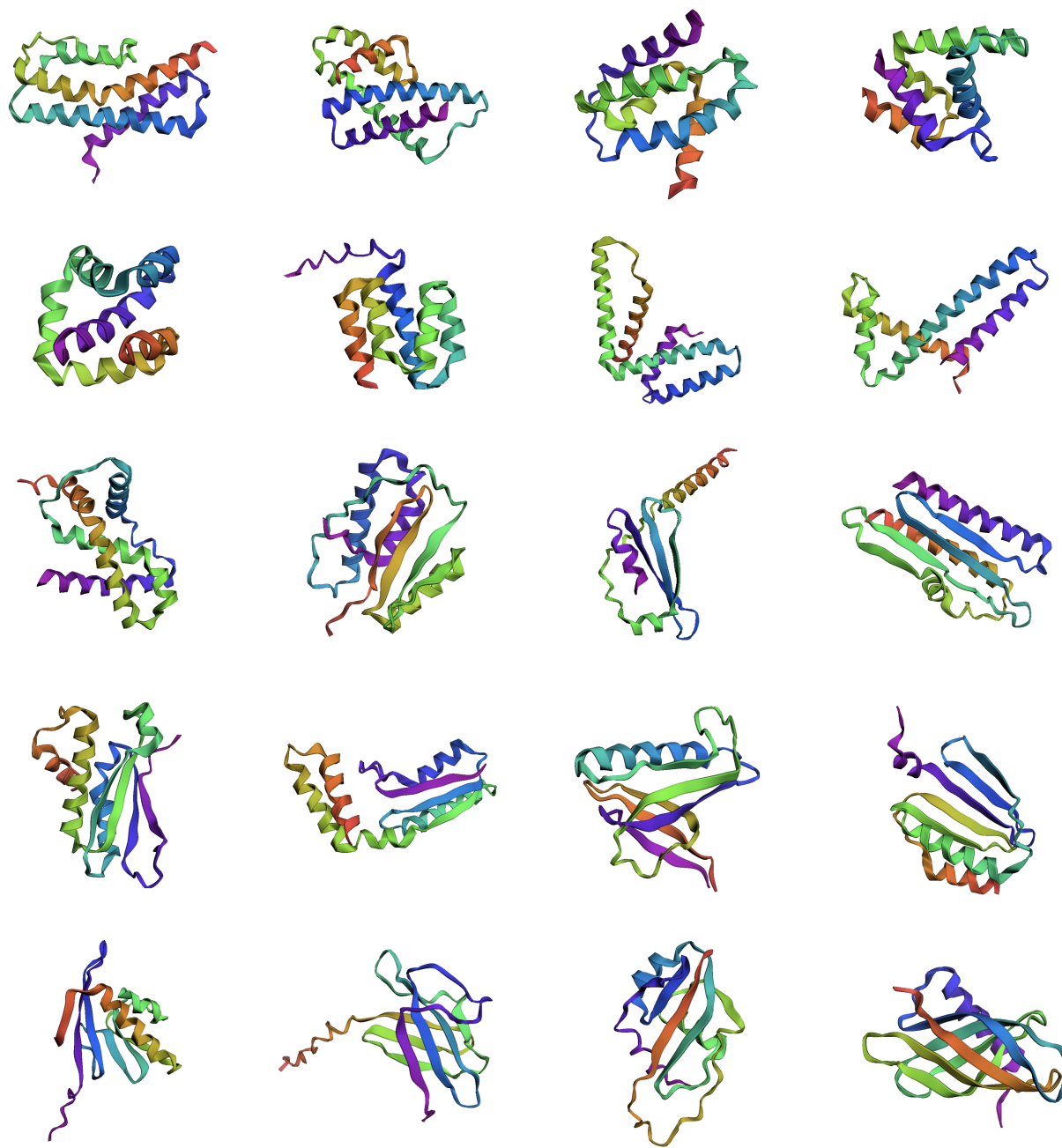


Figure 9. Additional examples of novel and confidently designable domains generated by Genie.